Stress Analysis of Composite Plates with Different Types of Cutouts

Dr. Riyah N.K.
Mechanical Engineering Department
University of Anbar

Mr. Ahmed N.E.
Mechanical Engineering Department
University of Anbar

Abstract
This research presents an experimental and theoretical investigation of the effect of cutouts on the stress and strain of composite laminate plates subjected to static loads. The experimental program covers measurement of the normal strain at the edges of circular and square holes with different number of layers and types of composite materials by using strain gages technique under constant tensile loads. A numerical investigation has been achieved by using the software package (ANSYS), involving static analysis of symmetric square plates with different types of cutouts. The numerical results include the parametric effects of lamination angle, hole dimensions, types of hole and the number of layers of a symmetric square plate. The experimental results show good agreement compared with numerical results. It is found that increasing the number of layers reduces the value of normal strain at the edges of circular and square holes of a symmetric plate and the maximum value of stress occurs at a lamination angle of (30^o) and the maximum value of strain occurs at a lamination angle of (50^o) for the symmetric square plates subjected to uni-axial applied load. The hole dimensions to width of plates ratio is found to increase the maximum value of stress and strain of a symmetric square plate subjected to uniaxial applied load. Moreover, the value of maximum stress increases with the order of type of circular, square, triangular and hexagonal cutout, whereas the value of maximum strain increases with the order of type of circular, square, hexagonal and triangular cutout.

Keywords: composite plate, stress analysis, laminate, cutout, numerical.

1. Introduction

The development of air and space vehicles with its peculiar requirements of structures which needed to be strong but light and flexible but tough, brought into a new breed of hybrid structural materials called reinforced composites. Fiber reinforced composite find increasing uses in aircraft and space vehicle structures, because of their high specific strength and stiffness properties, coupled with the flexibility in the selection of lamination schemes that can be tailored to match the design requirements [1]. Preliminary feasibility investigation, have revealed that the incorporation of high strength, high modulus glass or boron filaments in a low strength, low modulus and low density epoxy matrix can result in a composite material that offers the potential of a major break through in air and space vehicle design.

One of the first investigations in this field was reported by Forchet, M. M. [2], where the stress concentration factor for holes, grooves and fillets were determined by using different loading (pure tension, compression and bending) and using photo- elasticity method for determining the maximum value of stress from the change in photo-metric properties of certain solids due to the external load applied on the body under elastic conditions.

A thin plate of infinite extent containing a circular hole reinforced by uniformly thickening of one side of the plate in an annular region concentric with the hole subjected to an axially symmetric radial stress at infinity, has been solved by Wittrick [3,4]. Wittrick [3] obtained an asymptotic solution, valid for large stress at infinity and Wittrick [10] gave more general discussion of the axially symmetric problem, which contains an asymptotic solution for

the case when the added thickness is small. Waddoups [5] considered the problem of predicting the reduction in strength of a composite laminate static strength of composite laminate containing circular holes subjected to uniaxial loading which is reduced to a much higher degree than in metals where local stress redistribution due to plastic deformation may occur at the notch boundary. Conversely, notched strength of composite laminates is not reduced in proportion to the stress concentration factor.

Cherry [6] studied the elimination of fastener hole stress concentration through the use of softening strips. He estimated that static strength loss created by holes in boron/epoxy laminate amounts to approximately one-third in tension and one half in compression.

Richard et al. [7] presented the three-dimensional finite element analysis based on an isoparametric formulation for laminated composite in bending. The problem investigated was the laminate under uniform extension. Circular, square and diamond shaped holes of varying size were cut–out of the laminate. Stress concentration factors were defined for the tensile and inter-Laminar shear stresses were reported for both angle-ply and bi-directional laminates.

A boundary layer theory for isotropic elastic plates with circular cutout was extended for laminated composite by S. Tang [8]. An analytical solution was obtained for the extension of an infinite plate with a circular hole. The inter-laminar shear stresses and the normal or "peel" stress near and the edge of the hole were estimated for orthotropic plates. Numerical examples were given for $(0^{\circ}/90^{\circ})$ and $(\pm 45^{\circ})$ laminates plates.

The aim of the current work is to investigate experimentally the effect of opening (cutout) and number of layers of different types of composite materials on the normal strain at the edge of the hole of symmetric square plates. Moreover, theoretical work involves studying the effect of the following design parameters on the maximum stress and strain these design parameters are:

1-lamination angle (θ) of each layer. 2- The hole dimensions to width of plates ratio. 3-Number of layers. 4-Types of cutout.

2. Theoretical Considerations

The generalized Hooke's law relating stresses to strains for anisotropic materials can be written in contracted notation as [9]:

$$\sigma_i = C_{ij}\varepsilon_j \qquad i,j = 1,2,....,6 \tag{1}$$

The strains in contracted notation are defined as:

$$\varepsilon_1 = \frac{\partial u}{\partial x}, \quad \varepsilon_2 = \frac{\partial v}{\partial y}, \quad \varepsilon_3 = \frac{\partial w}{\partial z}, \tag{2}$$
$$\gamma_{12} = \frac{\partial v}{\partial x} + \frac{\partial u}{\partial y}, \quad \gamma_{23} = \frac{\partial v}{\partial z} + \frac{\partial w}{\partial z}, \quad \gamma_{13} = \frac{\partial u}{\partial z} + \frac{\partial w}{\partial x}$$

The elasticity matrix C_{ij} has 36 constants in Eqn.(1). However, an elastic potential or strain energy density function exists which implies [10]:

$$\begin{Bmatrix}\sigma_1\\ \sigma_2\\ \sigma_3\\ \sigma_4\\ \sigma_5\\ \sigma_6\end{Bmatrix}=\begin{bmatrix}C_{11} & C_{12} & C_{13} & C_{14} & C_{15} & C_{16}\\ & C_{22} & C_{23} & C_{24} & C_{25} & C_{26}\\ & & C_{33} & C_{34} & C_{35} & C_{36}\\ & & & C_{44} & C_{45} & C_{46}\\ & \text{symmetric} & & & C_{55} & C_{56}\\ & & & & & C_{66}\end{bmatrix}\begin{Bmatrix}\varepsilon_1\\ \varepsilon_2\\ \varepsilon_3\\ \varepsilon_4\\ \varepsilon_5\\ \varepsilon_6\end{Bmatrix} \tag{3}$$

If there is one plane of material property symmetry, the stress-strain relation reduced to:

$$\begin{Bmatrix}\sigma_1\\ \sigma_2\\ \sigma_3\\ \sigma_4\\ \sigma_5\\ \sigma_6\end{Bmatrix}=\begin{bmatrix}C_{11} & C_{12} & C_{13} & 0 & 0 & C_{16}\\ & C_{22} & C_{23} & 0 & 0 & C_{26}\\ & & C_{33} & 0 & 0 & C_{36}\\ & & & C_{44} & C_{45} & 0\\ & \text{symmetric} & & & C_{55} & 0\\ & & & & & C_{66}\end{bmatrix}\begin{Bmatrix}\varepsilon_1\\ \varepsilon_2\\ \varepsilon_3\\ \varepsilon_4\\ \varepsilon_5\\ \varepsilon_6\end{Bmatrix} \tag{4}$$

If there are two orthogonal planes of material property symmetry for a material, symmetry will exist relative to a third mutually plane. The stress-strain relations in coordinates aligned with principal material directions, (parallel to the intersections of the three plans of material symmetry) are:

$$\begin{Bmatrix}\sigma_1\\ \sigma_2\\ \sigma_3\\ \sigma_4\\ \sigma_5\\ \sigma_6\end{Bmatrix}=\begin{bmatrix}C_{11} & C_{12} & C_{13} & & & \\ C_{12} & C_{22} & C_{23} & \text{zeros} & & \\ C_{13} & C_{23} & C_{33} & & & \\ & & & C_{44} & & \\ & \text{zeros} & & & C_{55} & \\ & & & & & C_{66}\end{bmatrix}\begin{Bmatrix}\varepsilon_1\\ \varepsilon_2\\ \varepsilon_4\\ \varepsilon_5\\ \varepsilon_6\end{Bmatrix} \tag{5}$$

and are said to define an orthotropic material. Note that there is no intersection between normal and shearing stresses which occurs in anisotropic materials (by virtue of the presence of, for example, C_{14}). Similarly, there is no intersection between shearing stresses and normal strains as well as none between shearing stresses and shearing strains in different planes. Note also that there are now only nine independent constants in the elasticity matrix.

The principal directions of orthotropy often do not coincide with coordinate directions that are geometrically natural to the solution of the problem, as shown in **Fig. (1)**, [9]. Thus a relation is needed between the stresses and strains in the principal directions and those in body coordinates.

The transformation equations for expressing stresses in an *x-y* coordinate system in terms of stresses in a 1-2 coordinate system [9],

$$\begin{Bmatrix}\sigma_x\\ \sigma_y\\ \tau_{xy}\end{Bmatrix}=\begin{bmatrix}\cos^2\theta & \sin^2\theta & -2\sin\theta\cos\theta\\ \sin^2\theta & \cos^2\theta & 2\sin\theta\cos\theta\\ \sin\theta\cos\theta & -\sin\theta\cos\theta & \cos^2\theta-\sin^2\theta\end{bmatrix}\begin{Bmatrix}\sigma_1\\ \sigma_2\\ \tau_{12}\end{Bmatrix} \tag{6}$$

Similarly, the strain transformation equations are:

$$\begin{Bmatrix} \varepsilon_x \\ \varepsilon_y \\ \dfrac{\gamma_{xy}}{2} \end{Bmatrix} = \begin{bmatrix} \cos^2\theta & \sin^2\theta & -2\sin\theta c\cos\theta \\ \sin^2\theta & \cos^2\theta & 2\sin\theta\cos\theta \\ \sin\theta\cos\theta & -\sin\theta\cos\theta & \cos^2\theta - \sin^2\theta \end{bmatrix} \begin{Bmatrix} \varepsilon_1 \\ \varepsilon_2 \\ \dfrac{\gamma_{12}}{2} \end{Bmatrix} \tag{7}$$

If the laminate is thin, a line originally straight and perpendicular to the middle surface of the laminate which is assumed to remain straight and perpendicular to the middle surface when the laminate is extended and bent. Requiring the normal to the middle surface to remain straight and normal under deformation is equivalent to ignoring the shearing strains in planes perpendicular to the middle surface, that is, $\gamma_{xz} = \gamma_{yz} = 0$ where z is the direction of the normal to the middle surface in **Fig.(2)** [10]. In addition, the normals are presumed to have constant length so that the strain perpendicular to the middle surface is ignored as well, that is, $\varepsilon_z = 0$. The foregoing collection of assumptions of the behavior of the single layer that represents the laminate constitutes the familiar Kirchhoff-Love hypothesis for shells. Note that no restriction has been made to flat laminates.

The implications of the Kirchhoff or the Kirchhoff-Love hypothesis on the laminate displacements u, v, and w in the x-, y-, and *z*- directions are derived by using the laminate cross section in the *x*-*z* plane shown in **Fig.(2)**. The displacement in the *x*-direction of point B from the undeformed to the deformed middle surface is (u_o).

Since line ABCD remains straight under deformation of the laminate,

$$u_c = u_0 - z_c\beta \tag{8}$$

But since, under deformation, line ABCD further remains perpendicular to the middle surface, β is the slope of the laminate middle surface in the x-direction, that is,

$$\beta = \frac{\partial w_o}{\partial x} \tag{9}$$

Then, the displacement, u, at any point z through the laminate thickness is

$$u = u_o - z\frac{\partial w_o}{\partial x} \tag{10}$$

By similar reasoning, the v, in the y-direction is

$$v = v_o - z\frac{\partial w_o}{\partial y} \tag{11}$$

The laminate strains have been reduced to $\varepsilon_x, \varepsilon_y$, and γ_{xy} by virtue of the Kirchhoff-Love hypothesis. That is, $\varepsilon_z = \gamma_{xz} = \gamma_{yz} = 0$. For small strains (linear elasticity), the remaining strains are defined (after substituting the displacements u and v from Eqn.(10) and (11)) as follows:

$$\varepsilon_x = \frac{\partial u}{\partial x} = \frac{\partial u_o}{\partial x} - z\frac{\partial^2 w_o}{\partial x^2}$$
$$\varepsilon_y = \frac{\partial v}{\partial y} = \frac{\partial v_o}{\partial y} - z\frac{\partial^2 w_o}{\partial y^2} \qquad (12)$$
$$\gamma_{xy} = \frac{\partial u}{\partial y} + \frac{\partial v}{\partial x} = \frac{\partial u_o}{\partial y} + \frac{\partial v_o}{\partial x} - 2z\frac{\partial^2 w_o}{\partial x \partial y}$$

Thus, the Kirchhoff or Kirchhoff-Love hypothesis has been readily verified to imply a linear variation of strain through the laminate thickness. By substitution of the strain variation through the thickness, Eqn.(12), in the stress-strain relations, the stresses in the k^{th} layer can be expressed in terms of the laminate middle surface strains and curvatures as :

$$\begin{Bmatrix} \sigma_x \\ \sigma_y \\ \tau_{xy} \end{Bmatrix} = \begin{bmatrix} Q_{11} & Q_{12} & Q_{16} \\ Q_{12} & Q_{22} & Q_{26} \\ Q_{16} & Q_{26} & Q_{66} \end{bmatrix} \left\{ \begin{Bmatrix} \varepsilon_{ox} \\ \varepsilon_{oy} \\ \gamma_{oxy} \end{Bmatrix} + z \begin{Bmatrix} k_x \\ k_y \\ k_{xy} \end{Bmatrix} \right\} \qquad (13)$$

Since the Q_{ij} can be different for each layer of the laminate, the stress variation through the laminate thickness is not necessary linear, even though the strain variation is linear.

The resultant laminate forces acting on a laminate are obtained by integration of the stresses in each layer or lamina through the laminate thickness, as:

$$N_x = \int_{-h/2}^{h/2} \sigma_x dz \qquad (14)$$

Actually, N_x is a force per unit length (width) of the cross section of the laminate as shown in **Fig.(3)** [9]. The entire collection of force resultants for an N-layered laminate is defined as:

$$\begin{Bmatrix} N_x \\ N_y \\ N_{xy} \end{Bmatrix} = \int_{-h/2}^{h/2} \begin{Bmatrix} \sigma_x \\ \sigma_y \\ \tau_{xy} \end{Bmatrix}_k dz = \sum_{k=1}^{N} \int_{z_{k-1}}^{z_k} \begin{Bmatrix} \sigma_x \\ \sigma_y \\ \tau_{xy} \end{Bmatrix}_k dz \qquad (15)$$

Where z_k and z_{k-1} are defined in **Fig. (4)** [10]. Note that $z_0 = -h/2$, these forces resultants do not depend on z after integration, but are functions of x and y, the coordinates in the plane of the laminate middle surface.

The integration indicated in Eq.(15) can be rearranged to take advantage of the fact that the stiffness matrix for a lamina is constant within the lamina. Thus, the stiffness matrix goes outside the integration over each layer, but is within the summation of force and moment resultants for each layer. When the lamina stress-strain relations, Eq. (13), are substituted,

$$\begin{Bmatrix} N_x \\ N_y \\ N_{xy} \end{Bmatrix} = \sum_{k=1}^{N} \begin{bmatrix} Q_{11} & Q_{12} & Q_{16} \\ Q_{12} & Q_{22} & Q_{26} \\ Q_{16} & Q_{26} & Q_{66} \end{bmatrix}_k \left\{ \int_{z_{k-1}}^{z_k} \begin{Bmatrix} \varepsilon_{ox} \\ \varepsilon_{oy} \\ \gamma_{oxy} \end{Bmatrix} dz + \int_{z_{k-1}}^{z_k} \begin{Bmatrix} k_x \\ k_y \\ k_{xy} \end{Bmatrix} z dz \right\} \qquad (16)$$

However, it is noted that $\varepsilon_x^o, \varepsilon_y^o, \gamma_{xy}^o, k_x, k_y,$ and k_{xy} are not functions of z but are middle surface values so can be removed from under the summation signs. Thus, Eqn.(16) can be written as:

$$\begin{Bmatrix} N_x \\ N_y \\ N_{xy} \end{Bmatrix} = \begin{bmatrix} A_{11} & A_{12} & A_{16} \\ A_{12} & A_{22} & A_{26} \\ A_{16} & A_{26} & A_{66} \end{bmatrix} \begin{Bmatrix} \varepsilon_{ox} \\ \varepsilon_{oy} \\ \gamma_{oxy} \end{Bmatrix} + \begin{bmatrix} B_{11} & B_{12} & B_{16} \\ B_{12} & B_{22} & B_{26} \\ B_{16} & B_{26} & B_{66} \end{bmatrix} \begin{Bmatrix} k_x \\ k_y \\ k_{xy} \end{Bmatrix} \tag{17}$$

Where: $A_{ij} = \sum_{k=1}^{N} (Q_{ij})_k (z_k - z_{k-1})$ and: $B_{ij} = \frac{1}{2} \sum_{k=1}^{N} (Q_{ij})_k (z_k^2 - z_{k-1}^2)$ (18)

3. Experimental Work

Polyester resin, Glass fibers (E-glass woven & random) and carbon fibers have the properties shown in **Table (1)** [11]. Types of fibers include:

1. Two types of random glass fibers of weight per unit area of (420 and 360 gm/m^2).
2. Woven glass fibers of (280 gm/m^2) and the angle between fibers in the weave and weft direction is (0°/90°).
3. Woven carbon fibers of (220 gm/m^2) and the angle between fibers in the weave and weft direction is (0°/90°).

The specimens used in this study are prepared by hand–lay up molding for each type of reinforcement materials using mould with dimensions (20cm x 20cm x 2cm). Before pouring of the resin, mould surfaces should be dyed with chemically treated paraffin for the purpose of closing the spaces and to take the specimens easily from the mould. Then this material is modified with a piece of dwell and dye with an isolated material (tree-lack). This is a quickly dry soap liquid for the purpose of isolate the mould from the sample and can use the waxes to isolate the mould from the sample. After fibers arrangement inside the mould, the mixture (cobalt + polyester resins + hardener) is poured into the mould over the fiber and is stratified in layers. Then, the mould is left for (24) hours and the composite materials sheets are obtained.

The composite material is formed by using the procedure above and produced in hard and dry state forming a rectangular plate with (20cm x 20cm) dimensions and uniform thickness. Different types of fibers and number of layers can be used to produce many types of composite material with different thickness. Specimens with different thicknesses are cut first in equal rectangular form with 100mm length and 20mm width using iron scissors (cutter). The effective length of the specimen is 60mm, i.e. the ratio of (length/width) equal to (3). Circular and square holes are drilled with diamond – coated drill and dreamer sets by using a standard drill press and water cooling to avoid residuals stresses. The specimens used in this study are listed in **Table (2)**

There are two most important measurements for assessing the quality of a strain gauge installation. They are the insulation resistances between the gauge foil and specimen, and the shift in the gauge resistance due to installation process [12]. Linear strain-gauge type FLA-6-11, of the following characteristics is used in the present work:: Gauge length (6mm), Gauge resistance (120 ± 0-3), Gauge factor (2.12) and L.T No. (1527u). Digital strain meter is used to measure the strain. Tensile tests were conducted on universal testing machine of capacity (30kN) at laboratory temperature and with a load application speed equal to (0.0193 (mm/min).

4. Numerical Work

The dimensions of model used in (ANSYS) are (2a = 2b = 0.2 m), total thickness (0.006 m) and (D = 0.004 m), see **Fig. (6)**.

Material properties assigned , in studying of the effect of lamination angle (θ) , for low modulus graphite – epoxy [13] are: E_1= 132.3 GPa , E_2 = 10.7 GPa , G_{23} = 3.6 GPa , $G_{13} = G_{12}$ = 5.6 GPa , ν_{12} = 0.24.

Material properties assigned, in studying of the effect of (D/2b) ratio, for the boron – epoxy layers are [7]:
E_1 = 211 GPa , E_2 = 21GPa , $G_{12} = G_{13} = G_{23}$ =6.6 GPa , ν_{12} = 0.21.

5. Results and Discussion

Referring to **Table (3)**, the different values of weight/area of the two types of random glass fibers seem to have a negligible effect on the value of strain. This suggests that within the values of weight/area used the effect is diminished; should higher values be used the effect would be notable. The strain decreases appreciably as the number of layers increases; a logical result in view of the increased stiffness. Finally, it is noted that the strain near a square hole is greater than that near a circular hole, which manifests the effect of sharp corners on the stiffness of materials.

Figs. (7 through **16)** show the relation between the lamination angle (θ) and maximum stress and strain of the five symmetric square plates shown in **Fig.(6)** which consist of (4, 6, 8 and 12) layers of the same thickness.

In **Fig.(7)**, the maximum value of normal stress occurs at lamination angle of (30°), whereas the maximum value of strain seems to occur at lamination angle of (50°); the rate of change of strain with (θ) in the range (θ= 10^o-40^o) is high, see **Fig.(8)** . In the presence of a circular hole, as shown in **Fig. (9)**, the lamination angle has a little effect on the max. stress induced in plates consisting of (6) layers or more. For a square hole, there exist two values of critical angle of lamination of max. Stress occurrence, as shown in **Fig.(11)** . In general, the value of maximum stress increases with the order of type of circular, square, triangular and hexagonal cutout, whereas the value of maximum strain increases with the order of type of circular, square, hexagonal and triangular cutout.

Figs.(17-24) show the effect of (D/2b) ratio on the maximum stress and strain of the five symmetric square plates shown in Fig.(6) which consist of (4, 6, 8 and 12) layers of the same thickness.

The maximum value of normal stress increases with increasing of the (D/2b) ratio, and when (D/2b) ratio becomes more than (0.3) the change of maximum stress becomes very high in the range of (D/2b) ratio from (0.3-0.5); the maximum stress changes from (5.3-14.2) MPa. These results are only reasonable in view of the reduction in cross sectional area of the plate. The maximum strain value does not change linearly with increasing the (D/2b) ratio as shown in **Fig. (18)**. Also, the maximum value of strain, equal to ($360x10^{-6}$), occurs at (D/2b) ratio of (0.35); this means that the stiffness is decreased as the cutout dimensions are increased..

The shape of cutout affects the relation between both values of stress and strain with (D/2b) ratio. In case of square, hexagonal and triangular holes, the maximum stress occurs at (D/2b= 0.45, 0.4& 0.3) with values equal to (9.7, 26.4 & 24.3) MPa, as shown in **Figs. (19, 21** and **23)**. The maximum strain does not change linearly with increasing (D/2b) ratio for the case of square, hexagonal and triangular holes as shown in **Figs.(20 &24)** , but the maximum value of strain increases with increasing the (D/2b) ratio in a plate containing hexagonal hole as shown in **Fig.(22)** .

In all figures, increasing the number of layers results in reducing the maximum value of stress and strain for any given type or dimensions of cutout.

6. Conclusions

The following points may be concluded:

1. The value of normal strain at the edge of square hole is greater than the value at the edge of circular hole of a symmetric plate of different types of composite materials.
2. The type of fibers (random glass fibers, woven glass fibers and woven carbon fibers) does not affect the value of normal strain.
3. Increasing the number of layers decreases the maximum value of stress and strain of a symmetric square plate subjected to uni-axial applied load.
4. The maximum value of stress occurs at a lamination angle of (30^0) and the maximum value of strain occurs at a lamination angle of (50^0).
5. Increasing the hole dimensions to width of plates ratio increases the maximum value of stress and strain of a symmetric square plate subjected to uni-axial applied load.
6. The value of maximum stress increases with the order of type of circular, square, triangular and hexagonal cutout, whereas the value of maximum strain increases with the order of type of circular, square, hexagonal and triangular cutout.

7. References

[1] Moayad R. M., "Investigation of the transient response of composite laminated plates including the effect of cutout," M.Sc. Thesis, University of Baghdad, College of Eng., (2000).

[2] Forchet, M.M., "Photoelastic studies in stress concentration," Mechanical Engineering, Vol. 58, August (1936).

[3] W.H. Wittrik, "On the axisymmetric stress concentration at an eccentrically reinforced circular hole in a plate," Aeronautical Quarterly, 16, 15 (1965).

[4] W.H. Wittrik, "Axisymmetrical bending of a highly stretched annular plate," Quart., J. Mech. Appl. Math. 18, 11 (1965).

[5] Waddoups, M.E., Eisenmann, J.R. and Kaminski B.E., "Macroscopic fracture mechanics of advanced composite materials," J. Composite Material, vol. 5, pp. 446 – 454, October, (1971)

[6] Cherry, F.D., "The elimination of fastener hole stress concentration through the use of softening strips," Proceedings of The Conference on Fibrous Composite in Flight Vehicle Design), AFFDL – TR – 72 – 130, (1972).

[7] Richard M. Barker, Jon R. Dana and Charls, "Stress concentration near holes in laminates," J. Engineering of Mechanics Division, no. 10590, pp. 477 – 488, June (1974).

[8] S. Tang, "Inter-laminar stresses around circular cutouts in composite plate under tension," AIAA J. vol. 15, no. 11, pp. 1631 – 1637, November (1977).

[9] L.R. Calcote, "The Analysis of Lamination Composite Structures," Van Nostran Reinholed Company (1969).

[10] Robert M. Jones, "Mechanics of composite materials," McGraw-Hill Book Company, (1975).

[11] Hull, D, "An introduction to composite materials," University of Liverpool, Cambridge university, England, (1981).

[12] K.K. Ali, "Theoretical and experimental investigation of unsteady of forces on a cascade of axial flow compressor," M.Sc. Thesis, University of Baghdad, (2000).

[13] P. Bose & J.N. Reddy, "Analysis of composite plates using various plate theories. Part (2): Finite element model and numerical results," J. Structural Engineering and Mechanics, vol. 6, no. 7, pp. 727 – 746, (1998).

Nomenclature

A_{ij}	Extension stiffness elements
B_{ij}	Bending-extension coupling stiffness elements
C_{ij}	Element of elasticity matrix
N	Number of laminate layers
Q_{ij}	Transformed stress-strain relation from principal to laminate coordinates
Q_x, Q_y	Shear forces
N_i	Stress resultants
u,v,w	Displacements
u_o, v_o, w_o	Middle surface displacements
x,y,z	Rectangular coordinates
β	Slope of laminate middle surface
γ_{ij}	Shearing strain
γ_o	Middle surface shear strain
ε	Normal strain
ε_o	Middle surface strain
θ	Angle of lamination
σ	Normal stress
τ	Shearing stress

Table (1): Properties of materials used in the experiments.

Properties	Density (kg/m^3)	Young modulus (GN/m^2)	Poisson's ratio
Polyester	1.211	1.0602	0.38
E-glass	2.56	76	0.22
Carbon fiber	1.406	190	-

Table (2): Description of specimens used in experimental work.
Diameter or side length = 4mm, Total thickness =2 mm

Type of fibers	Weight/ area (gm/m^2)	Volume fraction of matrix	Volume fraction of fibers	No. of layers	Type of hole	Length to width ratio
RGF	420	0.45	0.55	4	Circular	3
RGF	420	0.42	0.58	4	Square	3
RGF	360	0.38	0.62	4	Circular	3
RGF	360	0.38	0.62	4	Square	3
RGF	420	0.46	0.54	8	Circular	3
RGF	420	0.35	0.65	8	Square	3
WCF+ WGF	220+880	0.43	0.57	5	Circular	3
WCF+ WGF	220+880	0.39	0.61	5	Square	3
WGF	280	0.41	0.59	8	Circular	2

Table (3): Experimental and numerical results of different types of composite materials

Type of Material	No. Layers	Type of hole	Strain (Experimental)	Strain (Numerical)	Discrep-ancy %(*)
Random[1]	4	Circular	0. 0189	0. 0177	6.35
Random[1]	4	Square	0. 019	0. 0209	10
Random[2]	4	Circular	0. 0191	0. 0226	18.3
Random[2]	4	Square	0. 0198	0. 0218	10.1
Random[1]	8	Circular	0. 0165	0.0142	14
Random[1]	8	Square	0. 0193	0.0183	5.18
Woven+ Carbon	5	Circular	0. 0118	0. 0101	14.4
Woven + Carbon	5	Square	0. 014	0. 0165	17.85
Woven	8	Circular	0. 011	0. 0125	13.63

$$(*)Discrepancy\ (\%) = \frac{\varepsilon_{x\,\mathrm{exp.}} - \varepsilon_{x\,num.}}{\varepsilon_{x\,\mathrm{exp.}}}$$

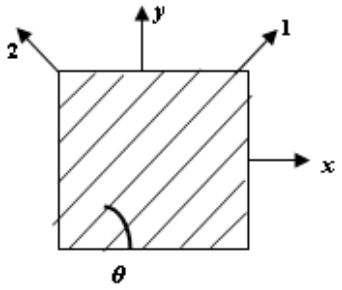

Figure (1): Lamina of arbitrary orientation of principal material

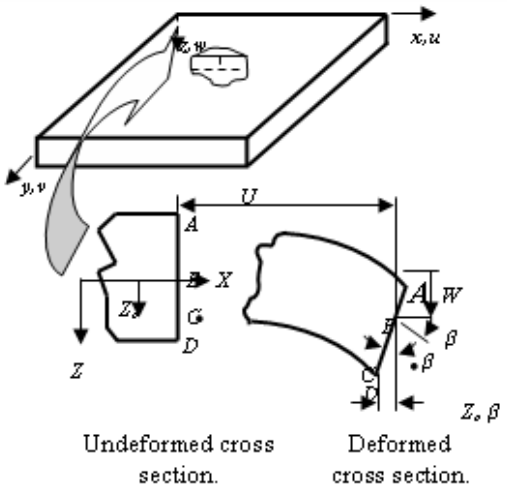

Figure (2): Deformation geometry in x-z

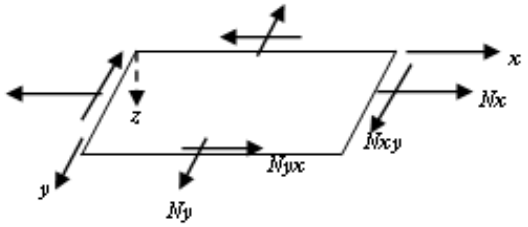

Figure (3): In-plane on a flat laminate

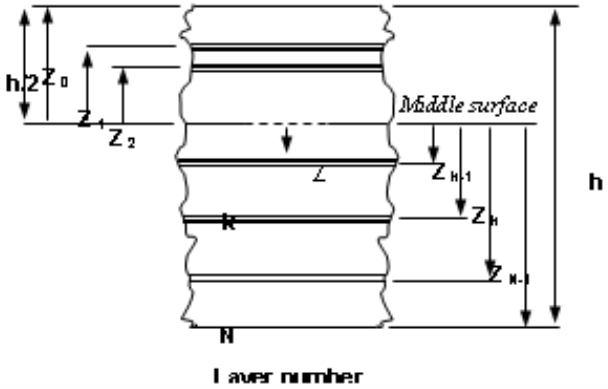

Figure (4): Geometry of an n-layered laminate[10].

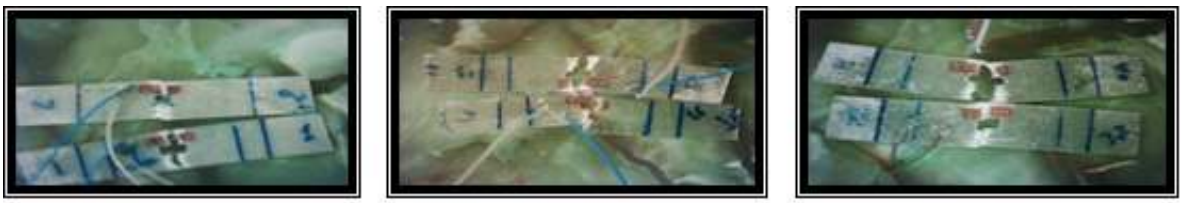

a: Random (1), 4-layers

b: Random (2), 4-layers

c: Random (1), 8-layers

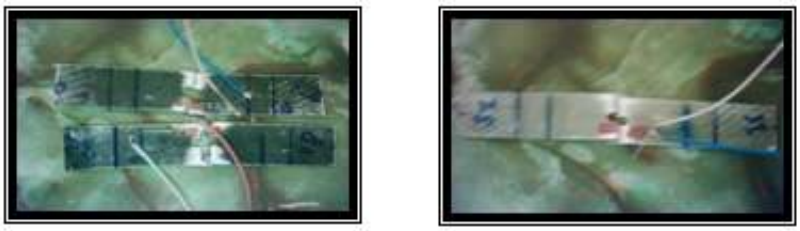

d: Woven glass – Woven carbon fibers 5- layers

e: Woven glass fibers 8-layers

Figure (5):Photographs of the specimens after testing.

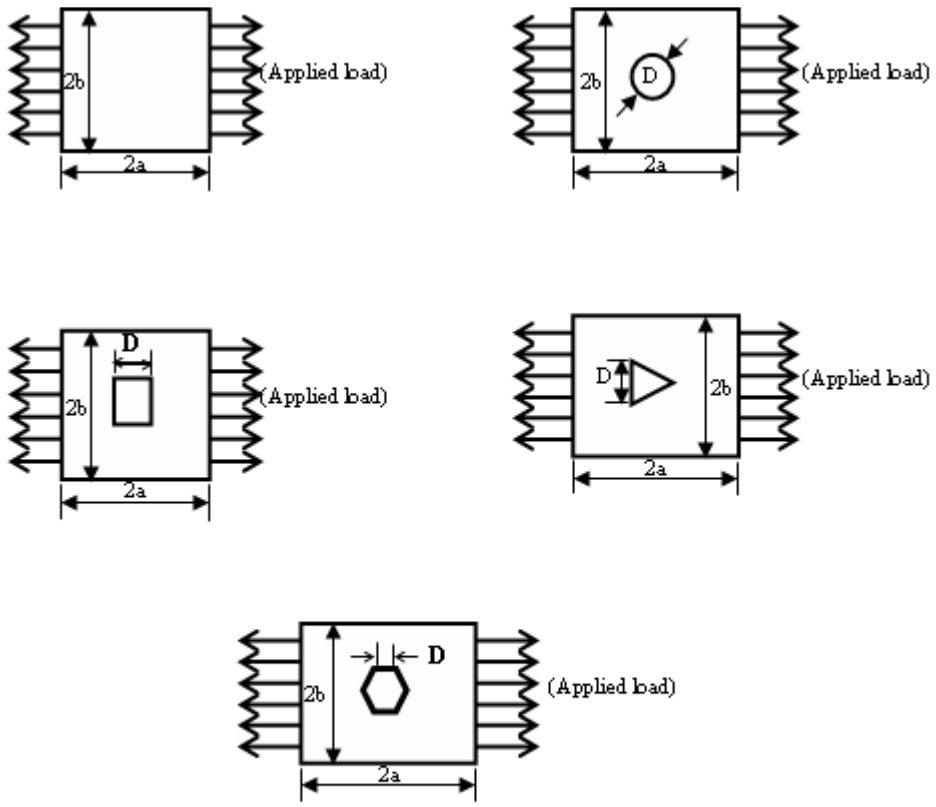

Figure (6): Square plates with different cutouts subjected to tension with central hexagonal hole subjected to tension.

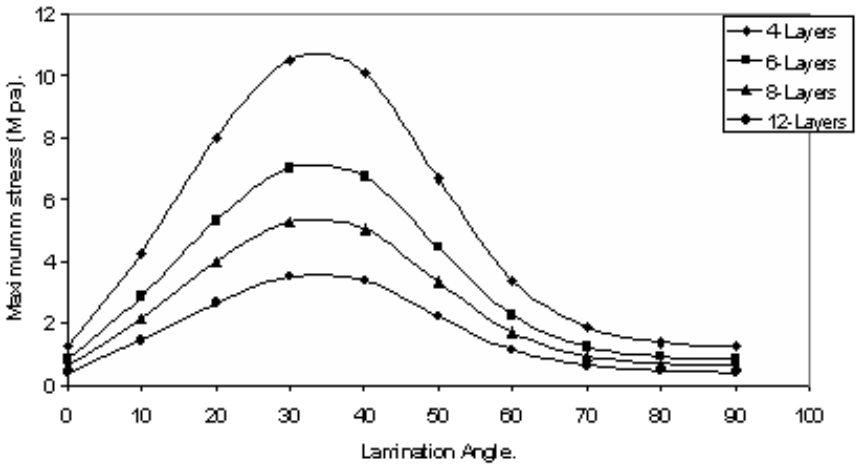

Figure (7):The effect of lamination angle on the maximum stress of asymmetric angle- ply laminates of a square plate .

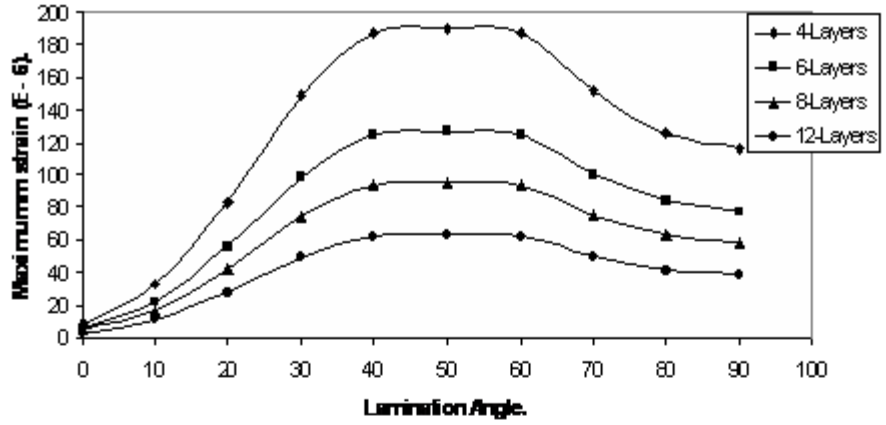

Figure (8): The effect of lamination angle on the maximum strain of asymmetric angle- ply laminates of a square plate.

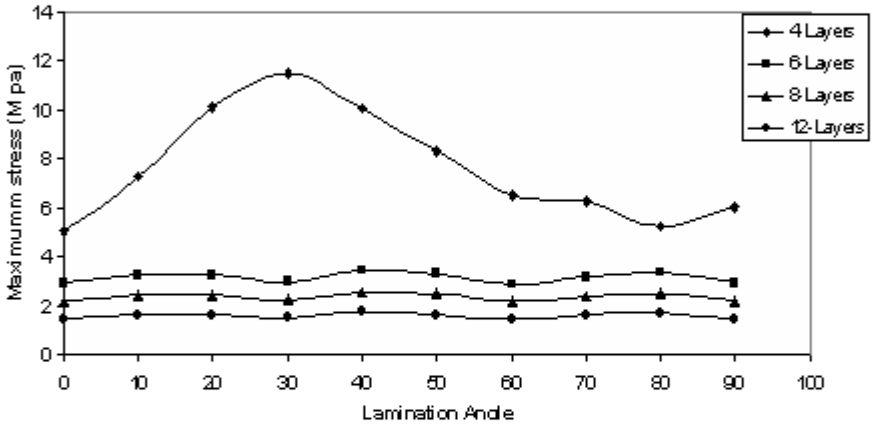

Figure (9): The effect of lamination angle on the maximum stress of asymmetric angle- ply laminates of a square plate with circular hole.

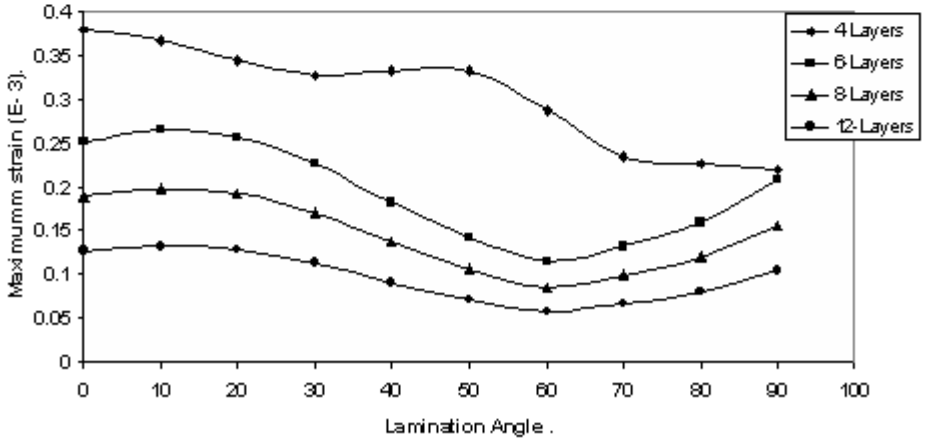

Figure (10): The effect of lamination angle on the maximum strain of asymmetric angle- ply laminates of a square plate with central circular hole.

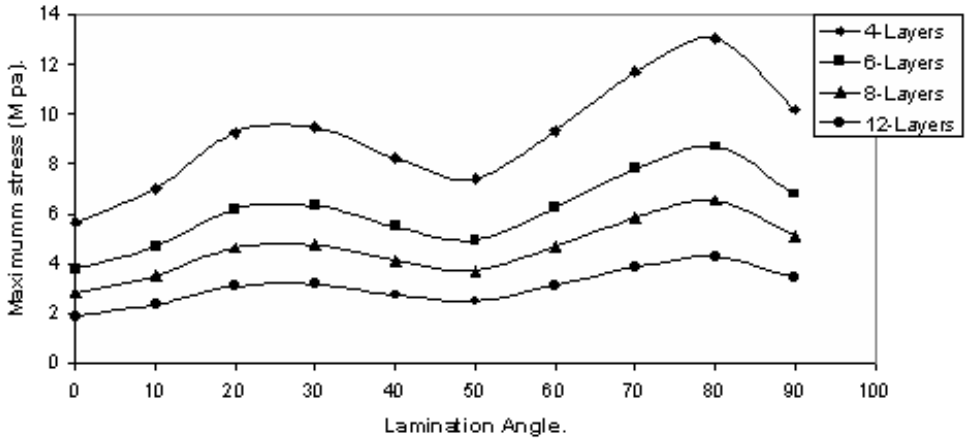

Figure (11): the effect of lamination angle on the maximum strain asymmetric angle-ply laminates of a square plate with central square hole

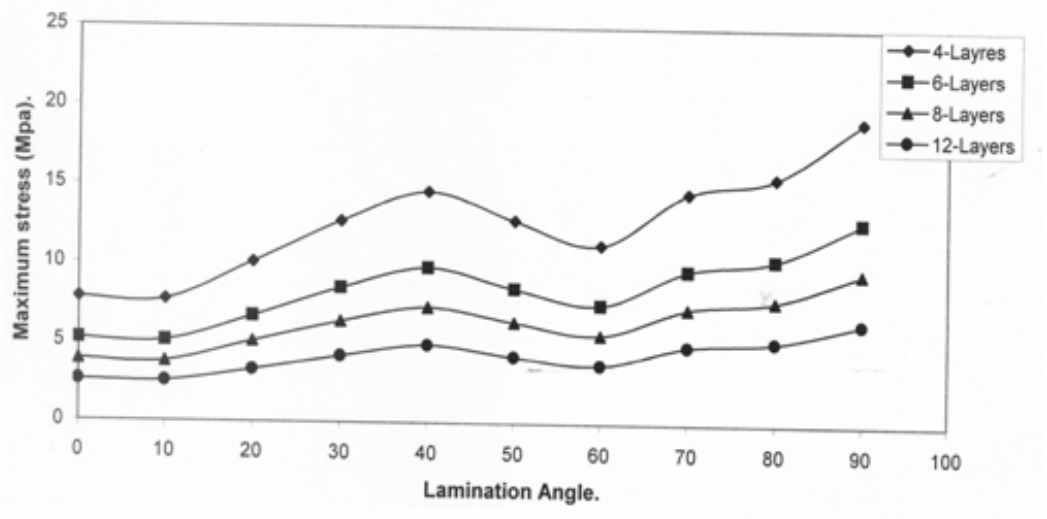

Figure (12): The effect of lamination angle on the maximum strain of asymmetric angle- ply laminates of a square plate with central square hole.

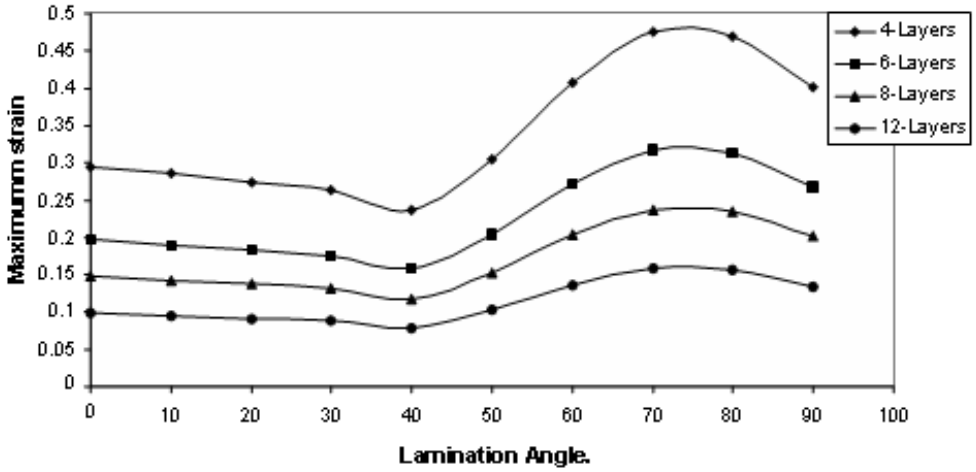

Figure (13): The effect of lamination angle on the maximum stress of asymmetric angle- ply laminates of a square plate with central hexagonal hole.

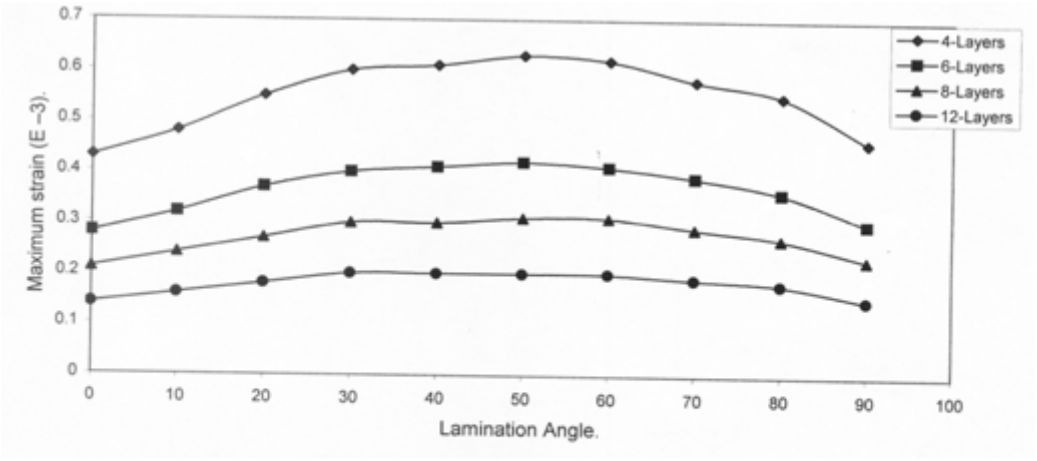

Figure (14): The effect of lamination angle on the maximum strain of asymmetric angle-ply laminates of a square plate with central hexagonal hole.

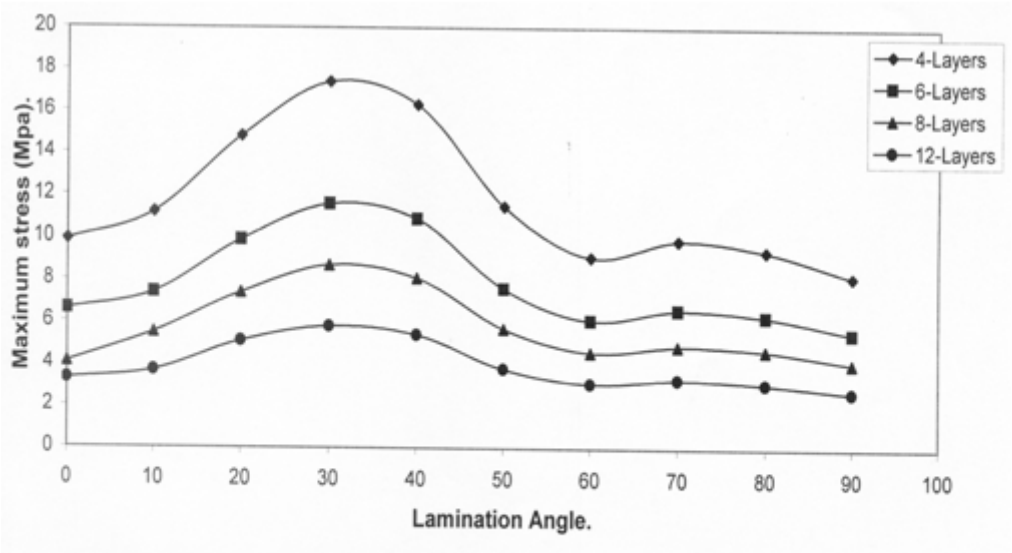

Figure (15): The effect of lamination angle on the maximum stress of asymmetric angle-ply laminates of a square plate with central triangular hole.

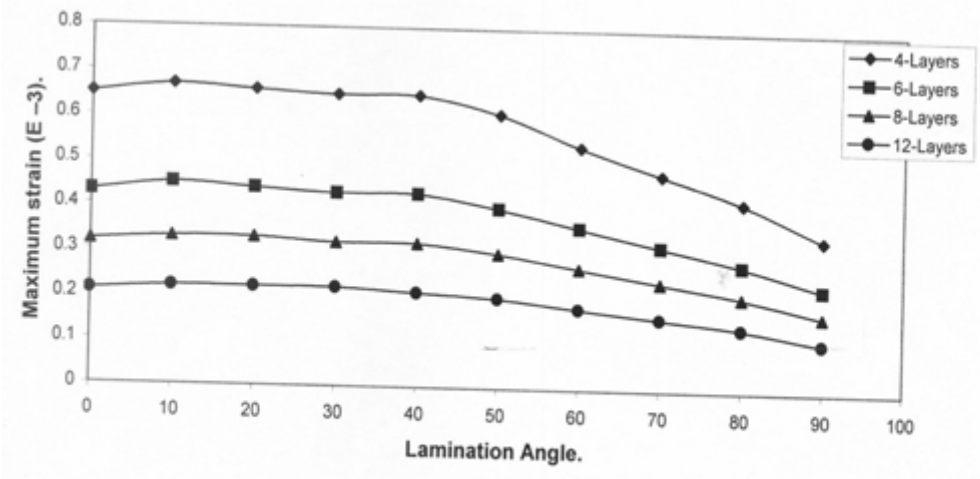

Figure (16): The effect of lamination angle on the max. Strain of asymmetric angle-ply laminates of a square plate with central triangular hole

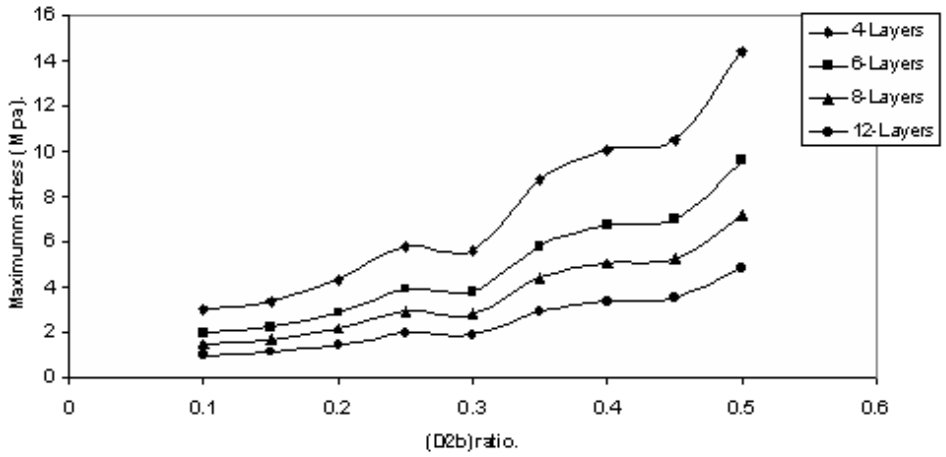

Figure (17): The effect of (D/2b) ratio on the maximum stress of asymmetric angle-ply laminates of a square plate with central circular hole.

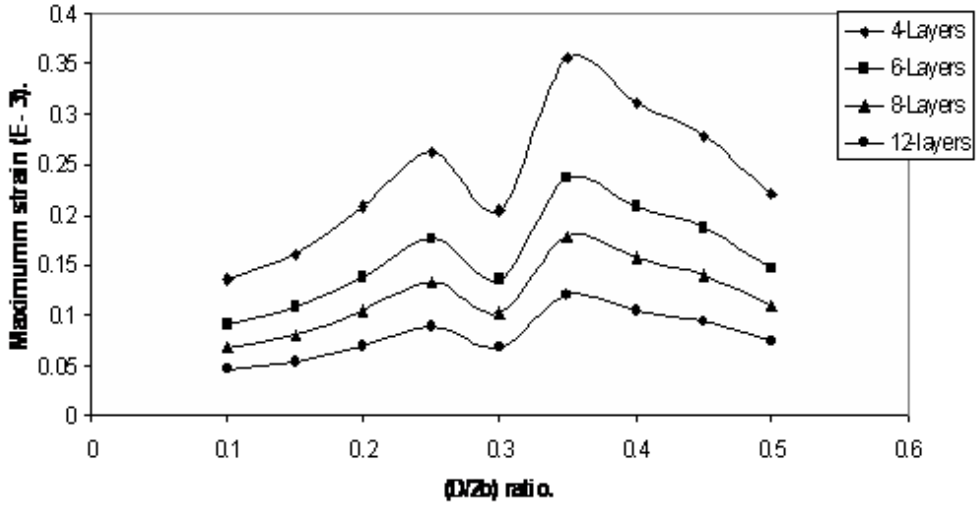

Figure (18):The effect of(D/2b) ratio on the maximum strain of asymmetric angle-ply laminates of a square plate with central circular hole.

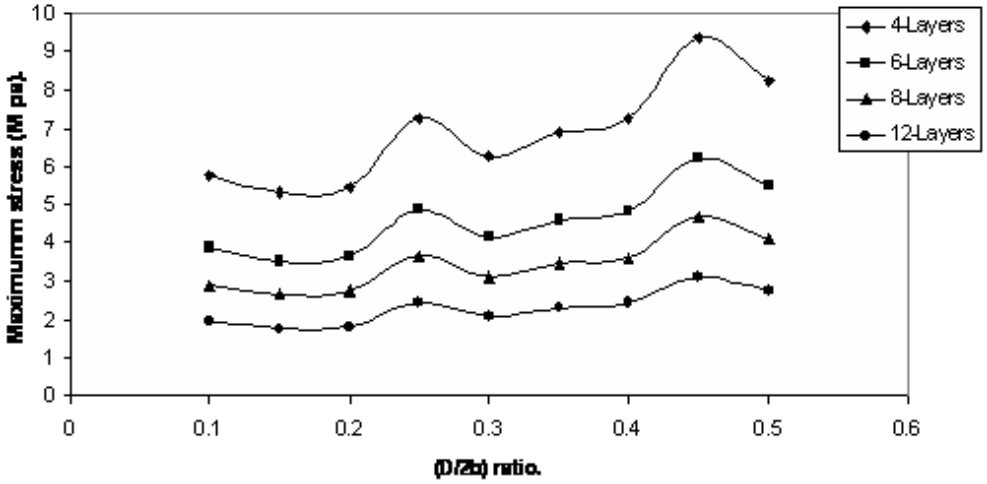

Figure (19):The effect of (D/2b) ratio on the maximum stress of asymmetric angle- ply laminates of a square plate with central square hole.

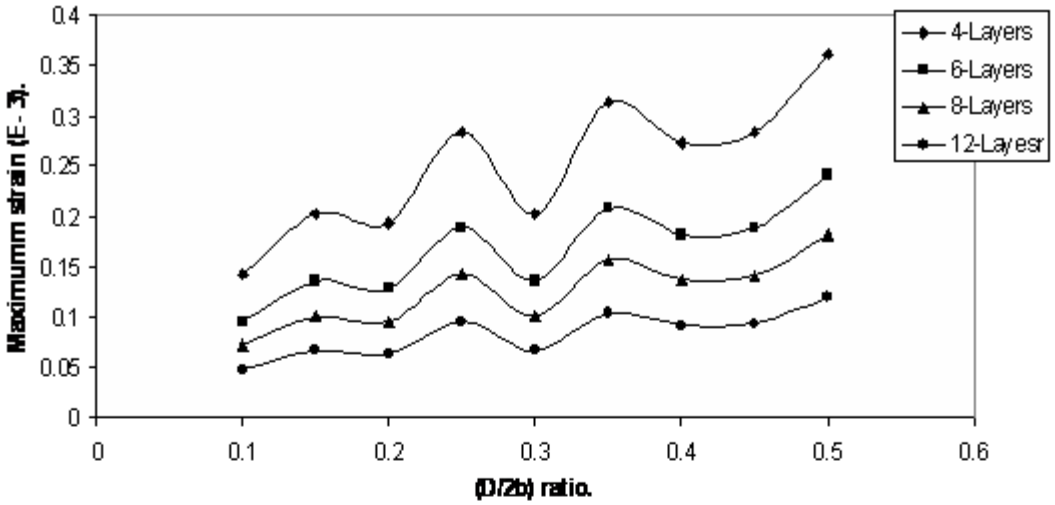

Figure (20):The effect of(D/2b) ratio on the maximum strain of asymmetric angle- ply laminates of a square plate with central square hole.

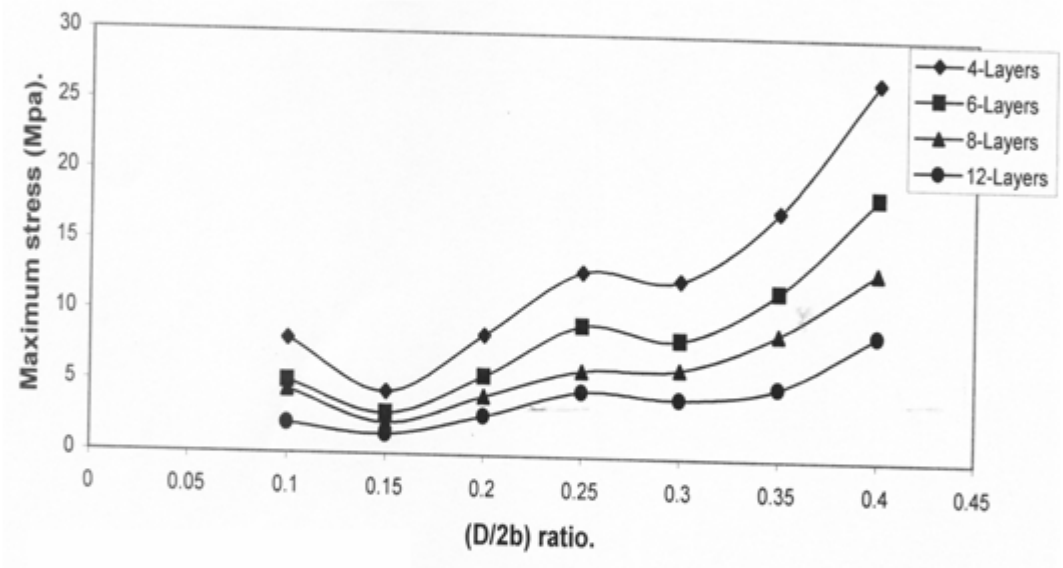

Figure (21):The effect of(D/2b) ratio on the max. Stress of asymmetric angle-ply laminates of a square plate with central hexagonal hole.

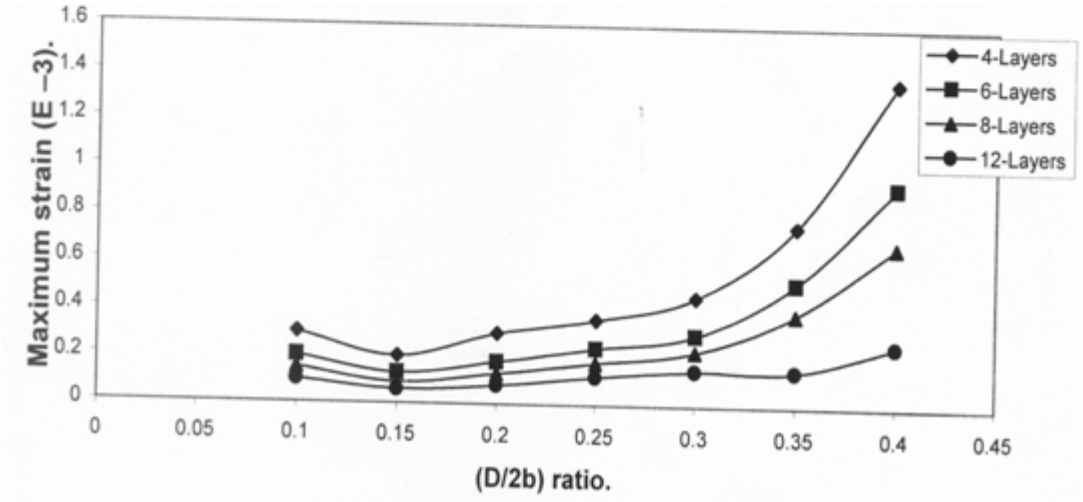

Figure (22):The effect of(D/2b) ratio on the max. Strain of asymmetric angle-ply laminates of a square plate with central hole. hhhexagonal hole.

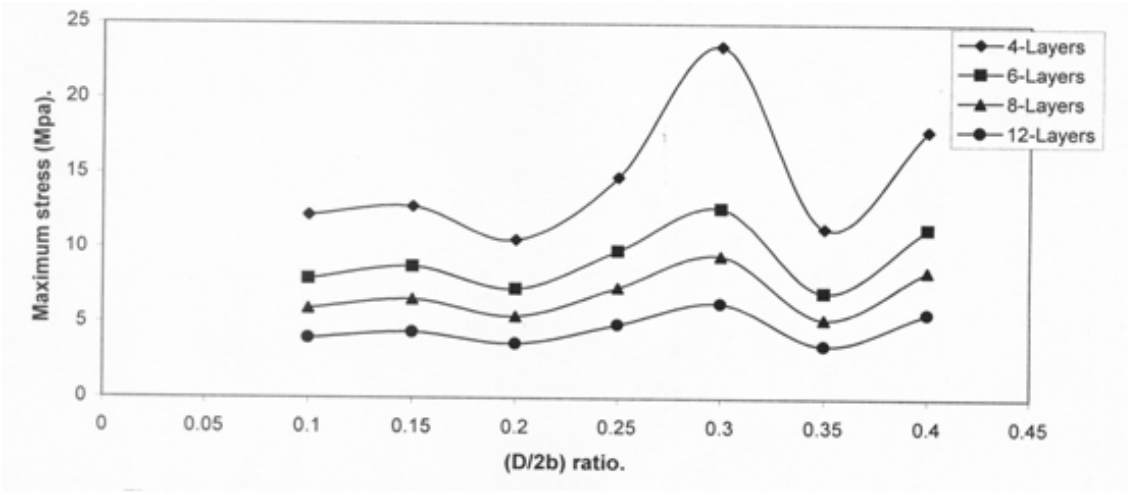

Figure (23):The effect of(D/2b) ratio on the maximum stress of asymmetric angle-ply laminates of a square plate with central triangular hole.

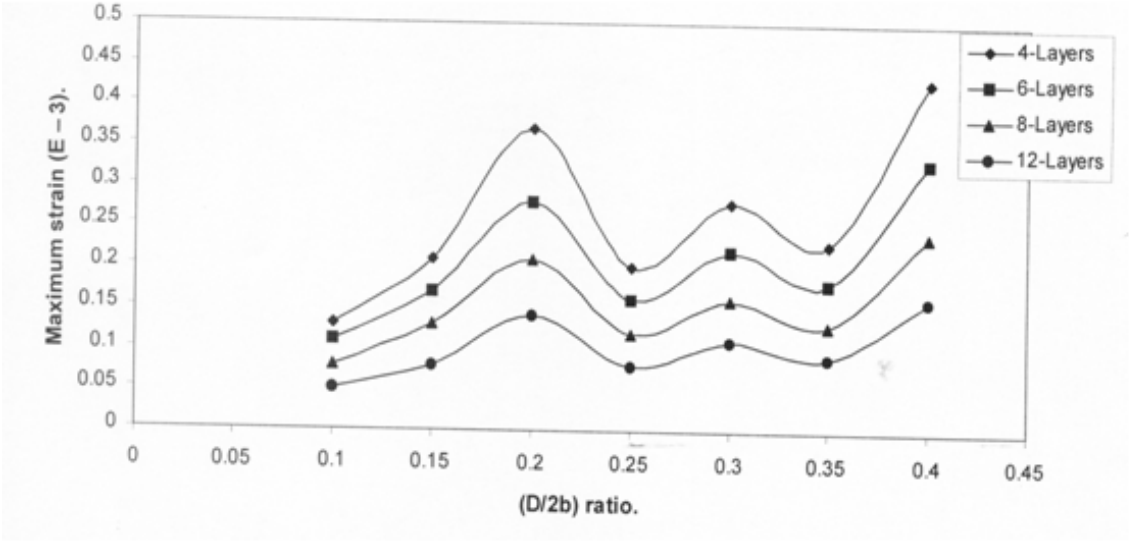

Figure (24):The effect of(D/2b) ratio on the maximum strain of asymmetric angle- ply laminates of a square plate with central triangular hole.

تحليل الاجهادات للألواح المركبة ذات الأنواع المختلفة من القطوعات

د.رياح نجم كطر
قسم الهندسة الميكانيكية / جامعة الانبار

السيد أحمد نوري عويد
قسم الهندسة الميكانيكية / جامعة الانبار

الخلاصة:

يتعرض هذا البحث لدراسة عملية و نظرية للألواح المركبة لإيجاد الاجهادات و الأنفعالات تحت تأثير الأحمال الأستاتيكية كذلك تم دراسة الألواح بوجود أجزاء مقطوعة للحصول على أمثل شكل للجزء المقطوع أي على أقل ما يمكن من الاجهادات و الأنفعالات المتولدة. تضمن الجزء العملي قياس الانفعالات عند حافة الثقوب (دائرية و مربعة) العمودية على اتجاه تسليط الأحمال (أحمال شد سكوني) للألواح المصنعة من عدد من الطبقات المختلفة و قد تم قياس الانفعالات باستخدام تقنية متحسسات الانفعال لغرض مقارنة بعض النتائج النظرية.تم انجاز الجزء النظري من هذا البحث باستخدام البرنامج الهندسي المعروف *(ANSYS)* الذي يعتمد طريقة العناصر المحددة. أن التحليل ألسكوني تمت دراسته للألواح المركبة التي تحتوي على أشكال مختلفة من الثقوب.أن النتائج التي تخص التحليل النظري تبين تأثير العوامل التصميمية المتمثلة في زاوية التركيب ، أبعاد الثقوب، عدد وسمك ونوع الطبقات الداخلة في تركيب الصفيحة. أن النتائج المستخلصة بالطريقة العملية أبدت توافق جيد مع النتائج النظرية. كما أستنتج أيضا بأن زيادة عدد الطبقات يقلل من قيمة الانفعال الطولي عند حافات الثقوب الدائرية والمربعة و كذلك فأن قيمة الإجهاد الأعظم يحدث عند الزاوية (30°)،قيمة الانفعال الأعظم يحدث عند الزاوية (50°).وجد ايضآ بان زيادة أبعاد الثقوب تزيد من الاجهادات والانفعالات كما وجد أن أعظم إجهاد يتزايد بتغيير شكل الثقب من دائري الى مربع إلى مثلث إلى سداسي وان أعظم انفعال يتزايد بتغيير شكل الثقب من دائري إلى مربع إلى سداسي إلى مثلث.